

Experimental investigation of the dynamics of a vibrating grid in superfluid ^4He over a range of temperatures and pressures

D. Charalambous,^{1,2,*} L. Skrbek,³ P. C. Hendry,¹ P. V. E. McClintock,¹ and W. F. Vinen⁴

¹*Department of Physics, University of Lancaster, Lancaster LA1 4YB, United Kingdom*

²*Meteorological Service, Ministry of Agriculture, Natural Resources and Environment, CY-1418 Nicosia, Cyprus*

³*Joint Low Temperature Laboratory, Institute of Physics ASCR, and Faculty of Mathematics and Physics, Charles University, V Holešovičkách 2, 180 00 Prague, Czech Republic*

⁴*School of Physics and Astronomy, University of Birmingham, Birmingham B15 2TT, United Kingdom*

(Received 11 February 2006; published 20 September 2006)

In an earlier paper [Nichol *et al.*, Phys. Rev. E, **70**, 056307 (2004)] some of the present authors presented the results of an experimental study of the dynamics of a stretched grid driven into vibration at or near its resonant frequency in isotopically pure superfluid ^4He over a range of pressures at a very low temperature, where the density of normal fluid is negligible. In this paper we present the results of a similar study, based on a different grid, but now including the temperature range where the normal fluid density is no longer insignificant. The new grid is very similar to the old one except for a small difference in the character of its surface roughness. In many respects the results at low temperature are similar to those for the old grid. At low amplitudes the results are somewhat history dependent, but in essence there is no damping greater than that *in vacuo*. At a critical amplitude corresponding to a velocity of about 50 mm s^{-1} there is a sudden and large increase in damping, which can be attributed to the generation of new vortex lines. Strange shifts in the resonant frequency at intermediate amplitudes observed with the old grid are no longer seen, however they must therefore have been associated with the different surface roughness, or perhaps were due simply to some artifact of the old grid, the details of which we are currently unable to determine. With the new grid we have studied both the damping at low amplitudes due to excitations of the normal fluid, and the dependence of the supercritical damping on temperature. We present evidence that in helium at low amplitudes there may be some enhancement in the effective mass of the grid in addition to that associated with potential flow of the helium. In some circumstances small satellite resonances are seen near the main fundamental grid resonance, which are attributed to coupling to some other oscillatory system within the experimental cell.

DOI: [10.1103/PhysRevE.74.036307](https://doi.org/10.1103/PhysRevE.74.036307)

PACS number(s): 47.27.Cn, 67.40.Vs, 47.15.Cb

I. INTRODUCTION

The study of turbulence in classical fluids has long provided us with many unsolved problems, which continue to attract researchers from a wide range of backgrounds, in engineering, mathematics, and physics. The study of turbulence in superfluid ^4He has also been active for many years, and studies of turbulence in other superfluids, formed in liquid ^3He or Bose-condensed atomic gases, have recently attracted much interest. Because superfluid turbulence can be strongly influenced by two-fluid behavior and by quantum restrictions in the flow of the superfluid component, it is often described as *quantum turbulence*. The quantum restrictions require that rotational motion be confined to quantized vortex lines, so that turbulence in the superfluid component takes the form of a more or less random tangle of these vortex lines [1,2].

Most of the many experimental investigations of turbulence in superfluid ^4He have been confined to temperatures above 1 K, where the inviscid superfluid component is accompanied by a significant fraction of viscous normal fluid. Although seemingly this two-fluid mixture might be thought to lead to rather complicated turbulent behavior, in practice it turns out in appropriate cases to be rather simple and similar to that found in classical fluids [3–5]. Nevertheless, it has

been clear that it would be of particular interest to study what must be a rather pure form of quantum turbulence: in a superfluid at temperatures low enough that there is no significant fraction of normal fluid. Unfortunately, such low temperature studies are technically difficult, partly because useful forms of mechanically driven flow at these temperatures are difficult to generate without excessive heating, and partly because second sound, which provides a powerful technique for the study of quantum turbulence at higher temperatures, ceases to be useful. Although efforts are in progress to build an acceptable mechanism for the generation of turbulence by a steadily moving grid at very low temperatures, the results of generating quantum turbulence at very low temperatures by other, simpler, methods have also been explored. These methods rely on the use of oscillating structures: in particular an oscillating levitated sphere in ^4He [6–9]; a vibrating wire in either ^4He or ^3He [10–14]; or a vibrating grid in either ^4He or ^3He [15,16,18,19]. In all cases the response of the structure to an oscillating drive can be used to study the dissipation due to the generation of turbulence; in the case of an oscillating grid in ^4He an attempt has been made to observe the turbulence by its effect in trapping negative ions; and in the case of ^3He the generated turbulence has been studied by Andreev scattering of quasiparticles. These studies suffer from two shortcomings: the generated turbulence inevitably lacks the simple homogeneity associated with a steadily moving grid; and comparisons

*Electronic address: demetris.c@physics.org

with classical analogs, which have been so important in studies of quantum turbulence at higher temperatures, are hampered by the shortage of relevant experiments on oscillating structures in classical fluids. Nevertheless, the results are proving to be interesting, and certain unexpected patterns of behavior are becoming apparent.

We ourselves have been concerned with the behavior of a circular stretched grid oscillating in its lowest mode in superfluid ^4He [15,16]. As in other cases the motion of the grid appeared to be essentially nondissipative at low amplitudes of oscillation, with an onset of dissipation at a critical velocity amplitude [17], which is typically about 50 mm s^{-1} . At high velocities the dissipative force appeared to be roughly proportional to the square of the grid velocity, which is reminiscent of classical behavior observed in steady flow past an obstacle at large Reynolds numbers [20]. At velocities below that at which there is onset of dissipation there were amplitude-dependent frequency shifts similar to those observed in a nonlinear oscillator [21], although behavior at these lower velocities was to some extent history-dependent. The shifts were to lower frequencies, by amounts much larger than the natural linewidth of the resonance, so that reentrant behavior was observed; and the shifts seem to set in at a critical velocity that was typically a factor of 10 less than that at which extra dissipation set in. Tentatively, we attributed these shifts to the nonlinear adiabatic response of loops of quantized vortex line attached to the grid, this adiabatic response giving rise to a nonlinear increase in the effective mass of the grid [22]. The existence of such remanent vortex loops is to be expected in superfluid ^4He , and they must be responsible for the (extrinsic) nucleation of turbulence that is associated with the onset of turbulent dissipation (intrinsic nucleation can occur only at much larger velocities). The two critical velocities (the “first and second thresholds”) depended differently on pressure, only the lower value being pressure-dependent.

These results were obtained with one particular grid. We recognized that the form and behavior of the remanent vortices might depend on the details of the surface roughness of the grid. In this paper we report results with a different grid, and we have included some study of the dependence not only on pressure but also on temperature. The experimental setup is briefly discussed in Sec. II but the reader is referred to [15] for more details. In Sec. III we present the experimental results followed by a discussion in Sec. IV. We draw conclusions in Sec. V.

A comparison of results obtained for our oscillating grids with those reported for oscillating spheres and wires reveals certain interesting similarities, in spite of the very different geometries: in particular very similar critical velocities and the existence of frequency shifts associated perhaps with enhanced effective masses. A full discussion of this comparison will be the subject of a future paper.

II. EXPERIMENT

The experimental setup is essentially identical to that described in Refs. [15,16]. The oscillating grid used in the measurements presented here was of exactly the same starting

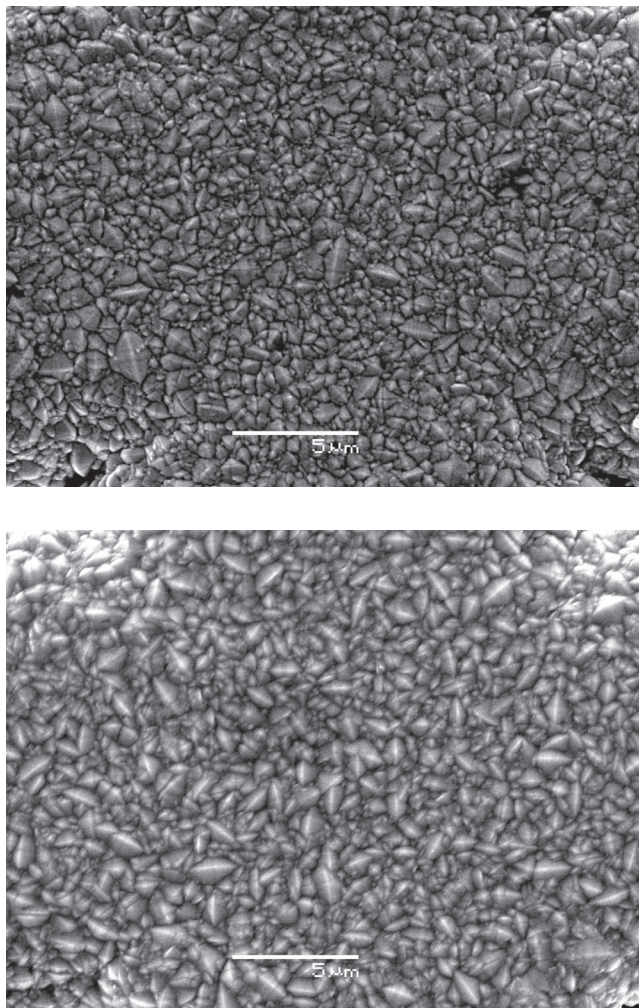


FIG. 1. Electron micrographs of the gold-evaporated grid used in Ref. [15] (top) and in the present measurements (bottom).

material, dimensions, and shape as the previous grid, but with slightly different tension and amount of gold evaporated on it. To the naked eye, the old grid appeared dull as compared to the much glossier, golden, new one. Shown in Fig. 1 are electron micrographs of these grids, for comparison. It can be seen that the surface quality of the two grids is similar, although the older grid appears to have a slightly finer texture.

As before, the grid was driven electrostatically by biasing it at a voltage of (usually) $V_0=536 \text{ V}$ and applying to an electrode placed 1 mm above the grid an oscillating voltage $V_1(t)=V_1^0 \cos(\omega t)$, where $V_1^0 \ll V_0$. Movement of the grid leads to an oscillating voltage V_2 induced in another electrode located at a distance $d=1 \text{ mm}$ directly below the grid, this voltage being measured with a Stanford Research SR-830 lock-in voltage amplifier. If we assume that the grid moves as a whole at right angles to its plane and use the fact that the input impedance of this amplifier is very large, we find that this voltage is given by $V_2=\alpha V_0 \Delta D/d$, where ΔD is the oscillation amplitude of the grid, and the factor $\alpha=[1+(C_c/C)]^{-1} \approx 0.063$ takes account of the stray capacitance C_c in parallel with the electrode system and associated with the cables and input to the amplifier. Details of the circuit are

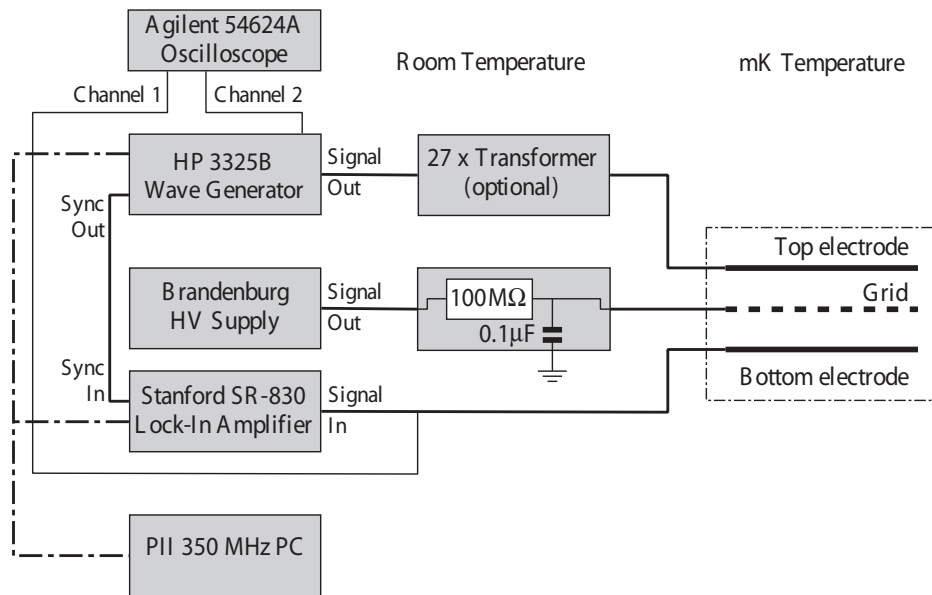


FIG. 2. Schematic circuit diagram indicating the various electrical connections to the experimental cell.

shown in Fig. 2. The lock-in amplifier measured the in-phase (V_1) and quadrature (V_2) responses of the grid; resonance curves reproduced later in this paper are plots of the amplitude $(V_1^2 + V_2^2)^{1/2}$.

The maximum speed of the grid, v , may be estimated roughly from the expression $v = \omega \Delta D$. However, a better estimate takes into account the shape and mode of oscillation of the grid. The grid is circular, of radius R , and is driven in its fundamental (0,1) mode, for which the displacement at radius r is given by the zero-order Bessel function of the first kind, $J_0(\alpha_0 r/R)$, where $\alpha_0 \approx 2.4048$ is the first zero of $J_0(x)$. The average displacement, in this case, is simply [23]

$$\left\langle J_0\left(\frac{\alpha_0}{R}r\right) \right\rangle = \frac{1}{\pi R^2} \int_0^{2\pi} d\phi \int_0^R dr r J_0\left(\frac{\alpha_0}{R}r\right) = \frac{2}{\alpha_0} J_1(\alpha_0) \approx 0.432.$$

Since $J_0(0)=1$, the maximum speed of the grid, which is at its center, may be estimated as $(1/0.432) \times \omega \Delta D \approx 2.3 \times \omega \Delta D$ [15].

III. EXPERIMENTAL RESULTS

A. Measurements *in vacuo*

The response of the grid was first measured *in vacuo*, before the experimental cell had been filled with helium. In order to minimize the risk of electrical breakdown, we applied in this case a relatively small bias to the grid (approximately 100 V), and a drive voltage of 0.1 Volt peak-to-peak (Vpp) to the upper electrode. Shown in Fig. 3 are a number of resonance characteristics of the grid, obtained during cooling from about 77 K to a base temperature, measured as about 8 mK inside the mixing chamber of the dilution refrigerator. While cooling the grid *in vacuo*, we are unable to obtain a reliable measure of its temperature because the ther-

mometers in the experimental cell are not then in good thermal contact with the grid.

The resonance curves marked “initial” correspond to a grid temperature close to 77 K. As the grid cools, its response settled to the well-defined resonance curve marked “final,” with a resonant frequency of 1036.9(1) Hz and a quality factor $Q \sim 4000$.

B. Measurements in He II: Zero temperature limit

Following these measurements *in vacuo*, the experimental cell was filled with isotopically pure ^4He (^3He molar fraction less than 10^{-13}) and pressurized to 5 bar. The response of the grid was then measured over a range of gradually increasing drive voltages, starting with the lowest available value

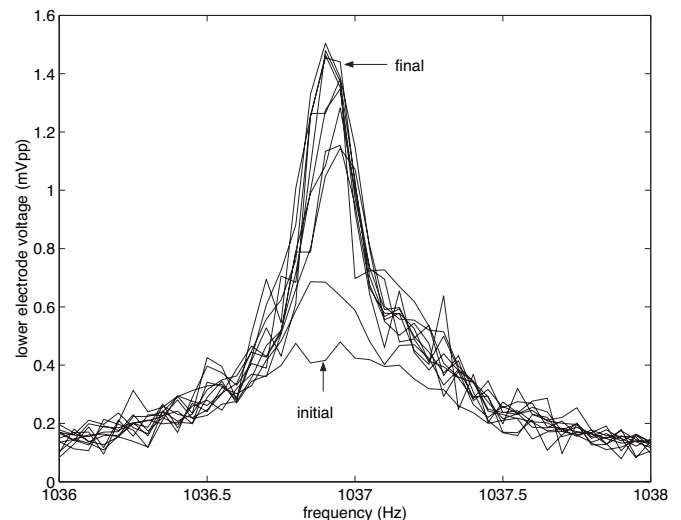


FIG. 3. Resonance characteristics of the grid obtained in vacuum during cooling from 77 K down to about 8 mK.

(1 mVpp), with typical results shown in Fig. 4(a).

The resonance curves are approximately Lorentzian in shape for low drive voltages, exhibiting a maximum at 997.90(5) Hz. However, the resonant frequency was found to shift suddenly to 998.02(5) Hz when the drive voltage reached 10 mVpp. Further shifts in resonant frequency, of order ± 0.1 Hz, were often seen in subsequent frequency scans. In order to suppress such changes in resonant frequency, the grid was “cleaned” before each new set of measurements (whenever, for example, the pressure in the cell was altered): a drive voltage of 10^4 mVpp (the highest available) was applied for a few seconds, followed by a measurement of the response at the lowest drive, until the latter remained unchanged. As we discuss later, we associate sudden changes in resonant frequency during the initial measurements with rearrangements of the remanent vortices on the grid, so that the “cleaning” procedure leads to a more stable arrangement of these vortices [15]. The behavior of the grid after “cleaning,” shown for a pressure of 5 bar in Fig. 4(b), will be referred to as *regular behavior*. It should be noted that the *initial* (irregular) *behavior* appears to be more pronounced at lower pressures. Figure 5 shows the *regular* resonance characteristics, obtained at a pressure of 10 bar and base temperature. Apart from a change in the resonant frequency (due, at least partly, to the change in the density of the liquid) these characteristics are very similar to those obtained at the lower pressure. An interesting feature of the data plotted in Fig. 5(b) is the existence of a small satellite peak in the vicinity of the main resonance peak; we comment on the origin of this parasitic resonance in Sec. IV. Similar behavior was observed at lower (2 bar) and higher (15 bar) pressures.

We see clearly in Figs. 4 and 5 that there is a sudden increase in resonant linewidth when the drive exceeds about 20 mVpp (corresponding to a critical speed of ~ 4 cm s $^{-1}$), in that the resonance curves then become almost flat-topped. We attribute this onset of extra dissipation due to vortex creation, or dissipative vortex motion, and the associated critical velocities are in agreement with those observed in our earlier experiments. The fact that this onset of nonlinear damping is not seen in the behavior of the grid when cold *in vacuo* confirms our assumption that the effect is associated with the helium and not with the grid itself or its supports.

C. Measurements in He II: Higher temperatures

The response of the vibrating grid was also measured as a function of temperature, at a fixed pressure. Shown in Fig. 6(a) are the resonance characteristics corresponding to a drive voltage of 10 mVpp, a pressure of 15 bar, and temperatures up to about 1.2 K. Also shown [Fig. 6(b)] is the corresponding variation of the resonance curve full width at half maximum (FWHM) with temperature. For temperatures exceeding 600 mK, the resonance characteristics are distorted by the parasitic resonance near 990 Hz. Hence the FWHM at these temperatures was *estimated* by doubling the half width at half maximum on the right of the resonance.

In Fig. 7(a) we show the response of the grid at resonance as a function of the driving voltage, for temperatures in the

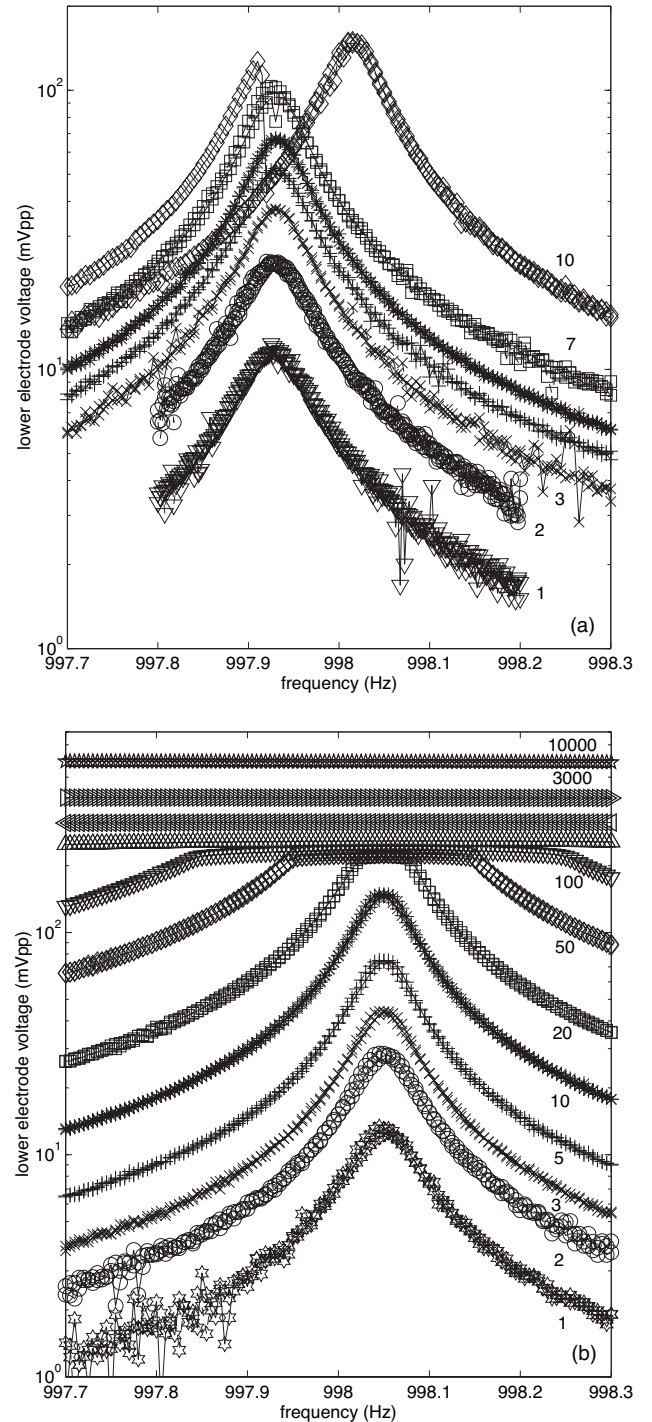


FIG. 4. Initial resonance characteristics as a function of applied driving voltage (a) obtained at a pressure of 5 bar, at base temperature. Shown in (b) are the corresponding resonance curves after the grid was “cleaned” (see text). Note that the resonance frequency of the grid in He II is shifted relative to that *in vacuo* by $\Delta f_0 \sim 40$ Hz.

range from 350 mK to 1.37 K, at a pressure of 15 bar. The onset of extra dissipation, to which we have already referred, is marked by a sudden change in slope of these curves. The curves can also exhibit an interesting hysteresis, as shown most clearly for a temperature of 500 mK in the lower inset.

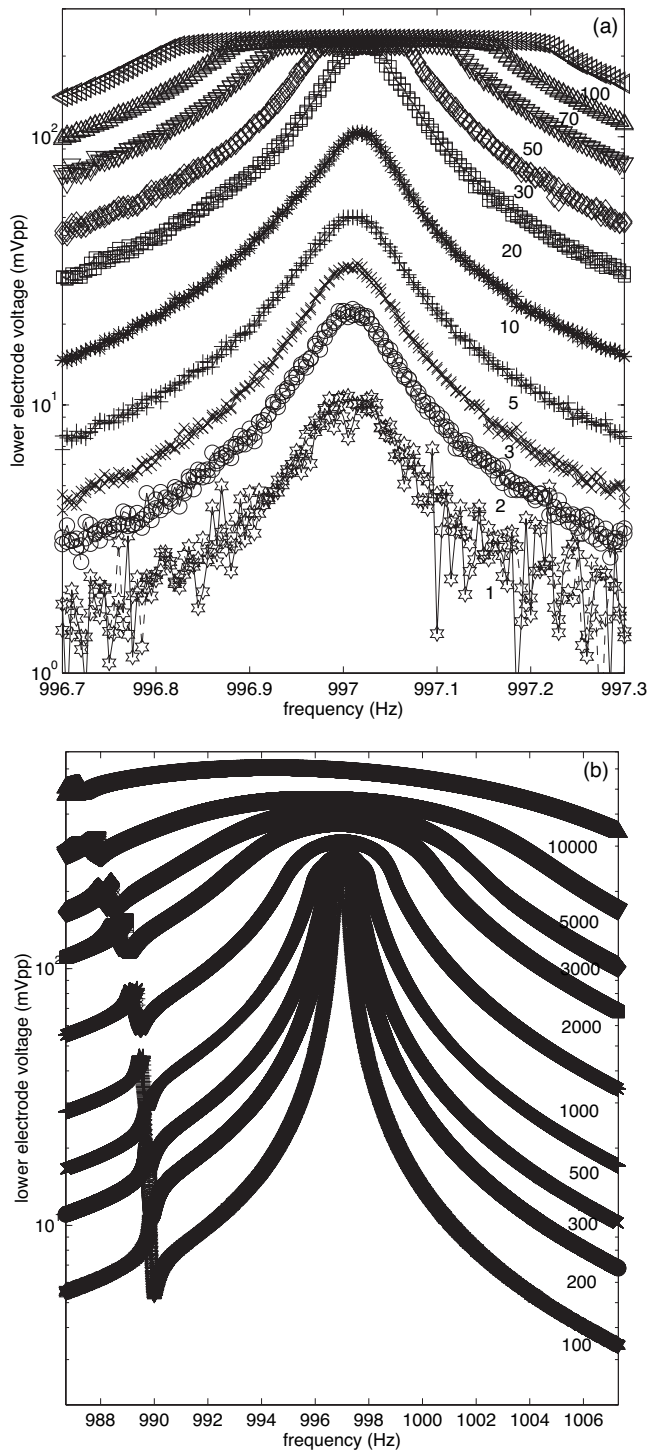


FIG. 5. (a) “Regular” resonance characteristics obtained at a pressure of 10 bar and base temperature, as a function of the applied drive voltage. Shown in (b) are higher-drive characteristics, plotted over a wider frequency range.

Note that the two “states” observed in this inset exhibit different damping, but in both cases the damping is linear with respect to the applied driving force. No such hysteretic effects were seen in the regular characteristics of the grid at

lower temperatures. Hysteresis is also observed in the resonance characteristics, as shown in Fig. 7(b). This effect requires further investigation. The critical grid velocity at which extra dissipation appears, derived from the data in Fig. 7, is plotted as a function of temperature in Fig. 8.

IV. DISCUSSION

A. Initial vs regular behavior

As shown in Sec. III B, when the experimental cell is first filled with liquid helium (or when the pressure in the cell is changed), the grid initially exhibits sudden changes in resonant response, this behavior being more pronounced at very low pressures. Similar effects were reported in our earlier work [15]. We believe that this behavior, which might also be called “virgin behavior,” is caused by rearrangement of remanent vortex lines. Such lines might be generated during filling of the experimental cell or simply be injected into the cell from the filling capillaries during pressure changes [24]. With the original grid, linewidths in the initial regime were larger than those in the regular regime, but this was not the case with the new grid.

After the cleaning procedure described in Sec. III B, the behavior of the grid becomes regular: the resonance frequency at the lowest drive (1 mVpp) remains constant within 0.01 Hz and the Q factor is of the order of 10^4 . As mentioned above and in earlier publications [15,16], this “cleaning” procedure is believed to lead to more stable arrangements of remanent vortex lines. The discussion that follows relates exclusively to the regular behavior.

B. Linear dissipation

In the presence of helium at the lowest temperatures, and at small amplitudes of oscillation, the observed damping of the grid is indistinguishable from that *in vacuo*. This residual damping must be associated with losses in the grid itself and in the grid mount, and we see that motion of the grid in the helium is without any extra frictional drag. At higher temperatures a linear damping appears, as shown in Fig. 6(b). This damping is due to an increasing fraction of thermally excited quasiparticles, or normal fluid. At temperatures below 1 K the mean free path of the quasiparticles is much larger than the mesh of the grid, and the dissipative drag arises from the ballistic scattering of the quasiparticles off the grid. This type of behavior was reported by Jäger *et al.* [6] for the case of an oscillating microsphere, and they showed that it leads to a drag coefficient that increases monotonically with temperature, in agreement with our own results [28,29]. At temperatures above 1 K the mean free path of the quasiparticles falls below the diameter of the wires in the grid, so that the damping can then be described in terms of a viscous drag. As in the measurements of Jäger *et al.*, this change leads to the maximum in the damping vs temperature that we observe in Fig. 6(b).

C. The onset of nonlinear dissipation

The sudden increase in linewidth that occurs when the drive exceeds about 20 mVpp must presumably be associ-

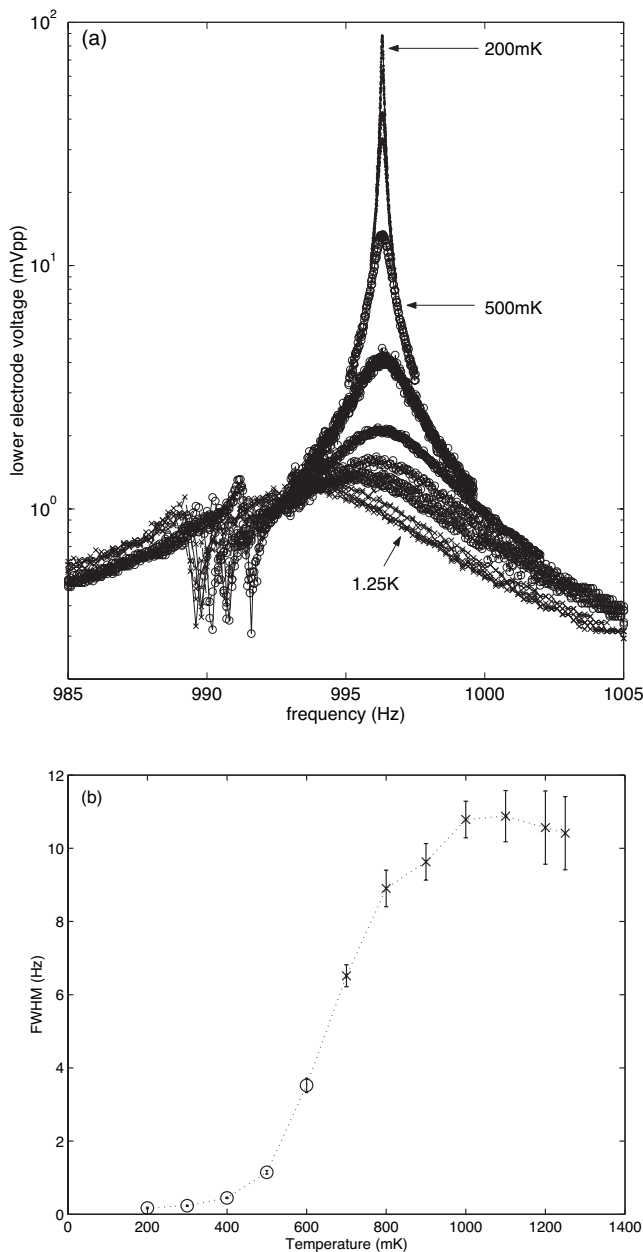


FIG. 6. Shown in (a) is the resonant response of the grid for various temperatures (200 mK to 1.25 K, top-to-bottom), for a drive voltage of 10 mVpp and a pressure of 15 bar. Graph (b) shows the variation of the linewidth (FWHM) of the resonance curves as a function of temperature. The values plotted with circle (○) markers were measured from the curves shown in the top graph, while those plotted with cross (×) markers represent estimates (see text).

ated with the dissipative motion of quantized vortices. This motion might take the form of a turbulent wake behind the grid, or it might, in principle, be associated with slippage in the phase of the superfluid order parameter due to the motion of vortex lines across the apertures in the grid. In the absence of any probe of turbulence behind the grid, we cannot distinguish between these two possibilities, although it seems reasonable to suppose that a turbulent wake must be involved at the higher velocities. The temperature dependence of the

critical velocity associated with the extra dissipation is shown in Fig. 8.

It is very interesting that critical velocities associated with the vibration of a single wire [12–14] or with the oscillation of a microsphere [6] are very similar in magnitude to those shown in Fig. 8, and that, at least qualitatively, there is a similar temperature dependence. This similarity exists in spite of the very different geometries, and in the case of wires it seems not to depend much on the surface roughness of the wire, in spite of the fact that this roughness might be expected to have a strong influence on any remanent vortices. We aim to return to a discussion of this potentially important similarity in a later paper.

D. Frequency shifts

In our Introduction we mentioned that in earlier experiments [15,16] with our first grid an amplitude-dependent frequency shift was observed at velocities below the critical velocity at which there is an increase in damping, and that this led to hysteretic “reentrant” resonance curves, characteristic of a nonlinear oscillator. No such behavior has been observed with the new grid, although small hysteretic effects can be seen in Fig. 7.

The large hysteresis has been tentatively attributed to a nonlinear adiabatic response of pinned remanent vortices to the oscillating flow of the superfluid through the grid [22]. Each pinned vortex must take the form of a vortex loop, each end of which is attached to the grid. Let $S(v)$ be the projection of the total area of these loops onto a plane perpendicular to the velocity of the grid; the area $S(v)$ was supposed to vary adiabatically with the average velocity v of the superfluid relative to the grid. Then it was shown [22] that the effective mass of the grid is given by

$$M_{\text{eff}} = M_0 + M_{\text{pot}} + \rho\kappa \frac{dS}{dv}, \quad (1)$$

where M_0 is the bare mass of the grid, and M_{pot} is the enhancement of its mass caused by potential flow through its structure (this is the well-known enhancement, associated with backflow, that occurs when a body moves through an ideal fluid [20]). We have assumed that the temperature is low, so that the superfluid density and the total density are equal in the last term. We have also assumed that the grid has adequate symmetry to ensure that its effective mass does not need to be represented as a tensor. If the area $S(v)$ is proportional to v , the adiabatic response of the remanent vortices leads to a constant enhancement of the effective mass, resulting in a constant shift in resonant frequency additional to that due to backflow. The shift in frequency with amplitude was supposed to result from a nonlinear dependence of $S(v)$ on v . If this is indeed the origin of the hysteretic resonance curves with our first grid, we must assume that in the second grid any remanent pinned vortices behave differently, for reasons associated perhaps with the slightly different form of surface roughness on the grid. But in reality we have no understanding of the different behavior of the two grids, and it may be due to some artifact of the old grid.

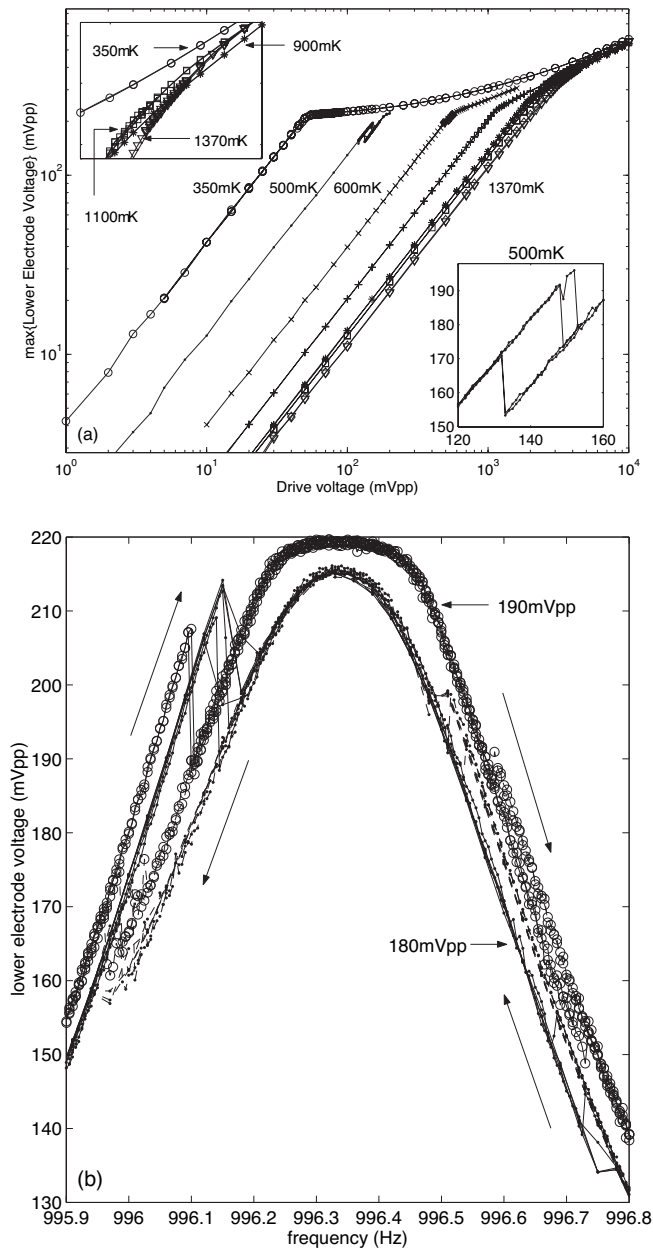


FIG. 7. Shown in (a) is the variation of the response at resonance as a function of the driving voltage, for a range of temperatures at a pressure of 15 bar. The lower inset shows part of the 500 mK plot, exhibiting hysteresis. Hysteresis also appears on the corresponding resonance characteristic, as shown in (b). The upper inset of (a) shows a closer view of the large drive region of the graph for selected temperatures.

There remains the possibility that with our second grid the remanent pinned vortices lead to an area $S(v)$ that remains proportional to v , so leading to a constant frequency shift in addition to that associated with potential flow (M_{pot}). For bodies of simple shape, the enhancement M_{pot} is easily calculated [20], but for a body with the shape of the grid this calculation is hardly possible with significant accuracy. Thus a comparison of the resonant frequencies with and without helium will not allow a distinction to be made between the

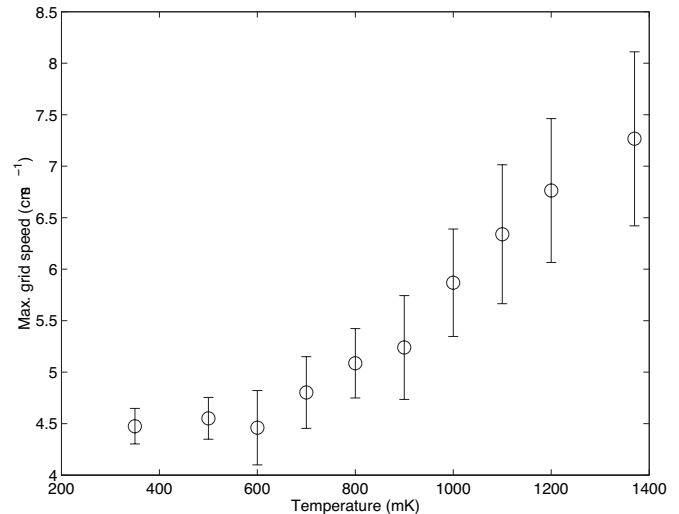


FIG. 8. The resonant response at the onset of dissipation (extracted from the data plotted in Fig. 7) as a function of temperature, at a pressure of 15 bar.

effect of potential backflow and that of an $S(v)$ that is proportional to v .

In considering whether there exists any constant contribution to the effective mass of the grid from the adiabatic response of the remanent vortices, we ask how the different contributions to the effective mass vary with the density of the helium and therefore with pressure [25]. The contribution from potential backflow is clearly proportional to the density. The density dependence of the term in $S(v)$ is less clear. If the detailed configuration of the remanent vortices were independent of density, then this last term would also be proportional to the density. However, it is likely that the configuration of remanent vortices is not independent of pressure, in which case the two contributions to the effective mass depend differently on density. We have tried to address this issue by examining how the resonant frequency, $f_1(\rho)$, of the grid, at low drives, is observed to vary with density. If the various contributions to the effective mass are proportional to density, then the quantity $1/f_1^2$ should be proportional to the density. We see in Fig. 9 that this relationship appears not to be obeyed; there appears to be a contribution to the effective mass that varies less strongly with density than that due to potential backflow (see particularly the inset to Fig. 9). We have checked that this effect is not associated with any irreversible change or damage to the grid, during cooling or during pressurization, by verifying that the resonant frequency of the grid at room temperature has suffered no change at the end of an experimental run. It should be noted, however, that further measurements are required in order to draw firm conclusions from the variation of resonance frequency with density: for instance, the vacuum point (corresponding to $\rho=0$) was measured by applying a lower bias voltage to the grid (~ 100 V as opposed to 536 V used in He II), in order to avoid electrical breakdown in the cell when no liquid helium is present. The resonance frequency of the grid could, potentially, depend on the bias voltage although having doubled the latter had no significant effect on the resonance frequency of the grid. This type of measurement is

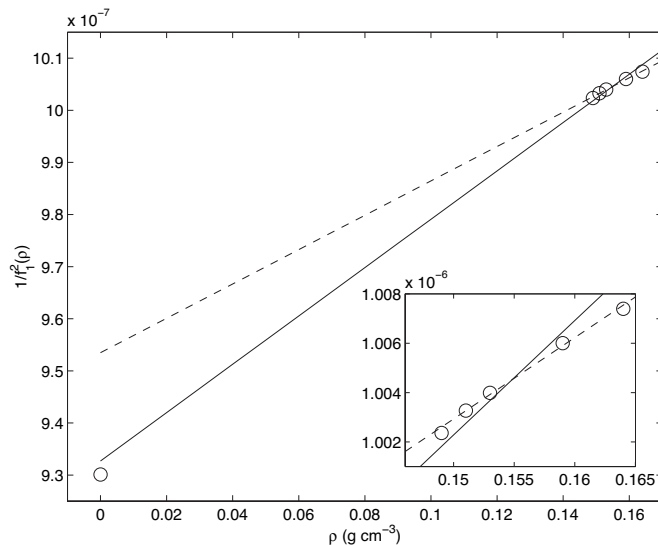


FIG. 9. The measured resonant frequency of the grid as a function of the density of He II at a drive of 1 mVpp); the value of density was extracted from the applied pressure using the data provided by Donnelly and Barenghi [26]. The dashed line is a straight-line fit to the points excluding the one at zero density; the continuous line is a similar fit taking into account all data points. The error bars are too small to show on this scale.

potentially very interesting and will be further explored in the future.

If there is indeed a contribution to the enhanced effective mass of the grid that is not proportional to the density, it might be due to the adiabatic response of remanent pinned vortices, although it might be associated with some other, as yet unknown, mechanism. It should also be recognized that, if the grid is coupled to another oscillatory system in the experimental cell, as we shall suggest in the next section as an explanation of the satellite peaks shown in Fig. 5(b), then this coupling can lead to a shift in the resonant frequency of the grid. Such a shift, depending on the density of the helium, might possibly account for the results in Fig. 9, although much further work would be required to establish whether or not this is the case.

In experiments on vibrating wires, the geometry of the wire is sufficiently simple to allow calculation of the effective mass enhancement due to potential backflow, so that measurements of the resonant frequency *in vacuo* and in helium at one pressure allows one to estimate rather easily the mass enhancement due to other effects. Yano *et al.* [13] have shown that such mass enhancements are observed and can be surprisingly large. However, these enhancements seem to vary with frequency and wire diameter in strange and perhaps not reproducible ways [27], and no enhancements have been observed by Bradley *et al.* [14], in spite of the fact that their wires were much more rough than those used by Yano *et al.* The experimental situation seems confusing, and further experimental work is required.

E. Satellite peaks

We have already pointed out the presence of satellite peaks in the resonance characteristics of the vibrating grid—

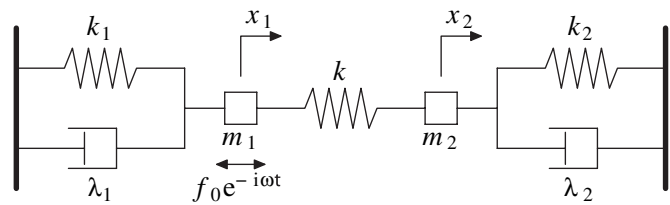


FIG. 10. A simple model comprising two, linearly coupled, harmonic oscillators, used to reproduce the experimental data containing satellite resonance peaks—see text for more details.

these can be clearly seen in Fig. 5(b) as well as in Fig. 6(a). It is highly unlikely that these peaks represent higher harmonics of the grid, as these would correspond to resonance frequencies which differ considerably from the observed ones. It is possible, however, that the satellite peaks arise as a result of coupling of the grid to another oscillator. Figure 10 illustrates a simple coupled oscillator model, where the grid system is represented by a mass m_1 , connected to a spring of spring constant k_1 and to a dashpot, providing a damping force of $\lambda_1 \dot{x}_1$, where x_1 is the displacement of m_1 from its equilibrium position (the dot represents differentiation with respect to time). The grid is driven by an oscillating force of the form $f_0 e^{-i\omega t}$. This system is now linearly coupled to another oscillator, with corresponding parameters m_2 , k_2 , and λ_2 , the coupling provided by a spring of spring constant k .

The equations of motion of the two masses are given by

$$m_1 \ddot{x}_1 + \lambda_1 \dot{x}_1 + k_1 x_1 + k(x_1 - x_2) = f_0 e^{-i\omega t},$$

$$m_2 \ddot{x}_2 + \lambda_2 \dot{x}_2 + k_2 x_2 + k(x_2 - x_1) = 0.$$

It is straightforward to show that the steady-state response X_1 of mass m_1 is given by

$$X_1 = \frac{f_0(k + k_2 - m_2 \omega^2 - i\omega \lambda_2)}{(k + k_1 - m_1 \omega^2 - i\omega \lambda_1)(k + k_2 - m_2 \omega^2 - i\omega \lambda_2) - k^2}.$$

Using the above expression, we managed to obtain very good agreement between one of the measured resonance characteristics of Fig. 5 (corresponding to 100 mVpp) and $|X_1|$, as can be seen from Fig. 11. The parameters which lead to the theoretical curve of Fig. 11 are $m_1=1, m_2=0.1176, \lambda_1=0.25, \lambda_2=0.0176, k_1=9.935 \times 10^5, k_2=1.149 \times 10^5, k=400$, and $f_0=10^5$. It can be seen that the coupling produces a shift in the resonant frequency of the grid of about 0.25 Hz; shifts of this magnitude would not be sufficient to account for the behavior shown in Fig. 9. However, other sets of parameters give equally good fits, and some of these other sets give much larger shifts.

Therefore the simple one-dimensional model of Fig. 10 is sufficient to reproduce all the characteristics of the satellite peak, including its shape, location, and size, as well as those of the main resonance peak (both in-phase and out-of-phase components). However, all one can conclude from this model is that the satellite peaks are likely to arise from coupling of the grid to another oscillator. These calculations do not reveal what this other oscillator is (apart from providing a possible set of parameters, such as effective mass, damp-

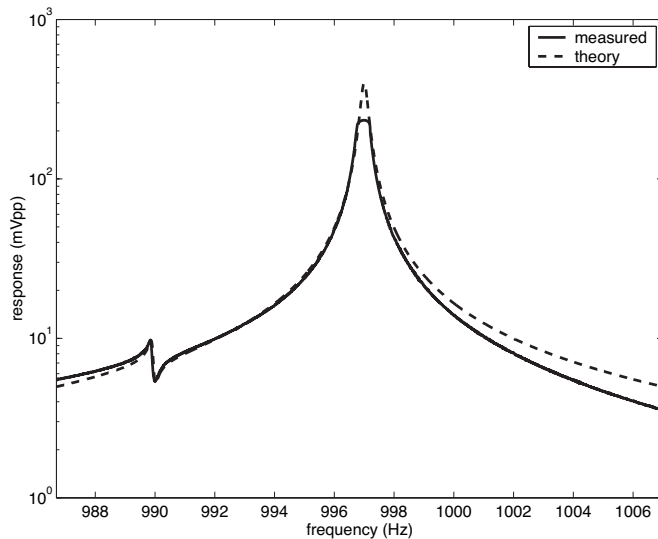


FIG. 11. The continuous line is the resonance characteristic shown in Fig. 5(b) for a drive voltage of 100 mVpp. The dashed line is the steady-state response of mass m_1 , of the coupled oscillator model shown in Fig. 10.

ing, etc.) and therefore further experimental tests are required in order to determine its origin. One possibility is that the oscillator is associated with an acoustic resonance in the experimental cell.

V. SUMMARY AND CONCLUSIONS

Our experimental results confirm various features observed earlier by us with a grid vibrating in superfluid ^4He at

a very low temperature. The new results are based on a grid that differs a little from the old one in the details of its surface roughness. The onset of dissipation at a critical velocity of about 50 mm s^{-1} , due presumably to vortex creation, is reproduced, but a dependence of the resonant frequency on amplitude of vibration at velocities below 50 mm s^{-1} is not seen. This latter effect must have been associated with the different surface roughness of the grid or was due to some unknown artifact of the old grid. The measurements with the new grid extend our knowledge of the damping of the grid at low velocities to higher temperatures, where it is caused by thermal excitations in the helium, and they allow us to measure the effect of temperature on the supercritical damping. There is some evidence that the effective mass of the grid at low velocities is larger than would be expected from potential flow, due perhaps to the adiabatic response of vortex loops pinned to the grid.

ACKNOWLEDGMENTS

We would like to express our gratitude to Tony Guénault for his invaluable assistance during these experiments and to Mark Giltrow for providing the gold evaporation apparatus and expertise. We are much indebted to Leanne Cooper and Nigel Fullwood who prepared the electron micrographs (Fig. 1) of the grid. We would also like to thank Shonah Ion, Steven Holt, and Andrew Muirhead for technical support. The research was supported by the Engineering and Physical Sciences Research Council (U.K.), by the Institutional Research Plan AVOZ10100520, and by the Czech Grant Agency under Grant No. GAČR 202/05/0218.

-
- [1] R. J. Donnelly, *Quantized Vortices in Helium II* (Cambridge University Press, Cambridge, 1991).
- [2] W. F. Vinen and J. J. Niemela, *J. Low Temp. Phys.* **128**, 167 (2002).
- [3] S. R. Stalp, L. Skrbek, and R. J. Donnelly, *Phys. Rev. Lett.* **82**, 4831 (1999).
- [4] L. Skrbek and S. R. Stalp, *Phys. Fluids* **12**, 1997 (2000).
- [5] W. F. Vinen, *Phys. Rev. B* **61**, 1410 (2000).
- [6] J. Jäger, B. Schuderer, and W. Schoepe, *Phys. Rev. Lett.* **74**, 566 (1995).
- [7] M. Niemetz, H. Kerscher, and W. Schoepe, *J. Low Temp. Phys.* **126**, 287 (2002).
- [8] M. Niemetz and W. Schoepe, *J. Low Temp. Phys.* **135**, 447 (2004).
- [9] W. Schoepe, *Phys. Rev. Lett.* **92**, 095301 (2004).
- [10] T. Morishita, T. Kuroda, A. Sawada and T. Satoh, *J. Low Temp. Phys.* **76**, 387 (1989).
- [11] D. I. Bradley, *Phys. Rev. Lett.* **84**, 1252 (2000).
- [12] H. Yano, A. Handa, H. Nakagawa, K. Obara, O. Ishikawa, T. Hara, and M. Nakagawa, *J. Low Temp. Phys.* **138**, 561 (2005).
- [13] H. Yano, A. Handa, M. Nakagawa, K. Obara, O. Ishikawa and T. Hata, in *Proceedings of the 24th International Conference on Low Temperature Physics* (AIP, Melville, NY, 2006), pp. 195–198.
- [14] D. I. Bradley, D. O. Clubb, S. N. Fisher, A. M. Guénault, R. P. Haley, C. J. Matthews, G. R. Pickett, and K. Zaki, *J. Low Temp. Phys.* **138**, 493 (2005).
- [15] H. A. Nichol, L. Skrbek, P. C. Hendry, and P. V. E. McClintock, *Phys. Rev. E* **70**, 056307 (2004).
- [16] H. A. Nichol, L. Skrbek, P. C. Hendry, and P. V. E. McClintock, *Phys. Rev. Lett.* **92**, 244501 (2004).
- [17] Grid velocity values refer to the peak velocity of the grid at its center. Note that the velocity figures which appear in Table II of Ref. [15] refer to the peak *flow* velocity, which is equal to the peak velocity of the grid at its center multiplied by the grid transparency factor.
- [18] D. I. Bradley, D. O. Clubb, S. N. Fisher, A. M. Guénault, R. P. Haley, C. J. Matthews, G. R. Pickett, V. Tsepelin, and K. Zaki, *Phys. Rev. Lett.* **95**, 035302 (2005).
- [19] D. I. Bradley, D. O. Clubb, S. N. Fisher, A. M. Guénault, R. P. Haley, C. J. Matthews, G. R. Pickett, V. Tsepelin, and K. Zaki, *Phys. Rev. Lett.* **96**, 035301 (2006).
- [20] L. D. Landau and E. M. Lifshitz, *Fluid Mechanics* 2nd ed. (Butterworth-Heinemann, Oxford, 1984).
- [21] L. D. Landau and E. M. Lifshitz, *Mechanics*, 3rd ed. (Butterworth-Heinemann, Oxford, 1983).

- [22] W. F. Vinen, L. Skrbek, and H. A. Nichol, *J. Low Temp. Phys.* **135**, 423 (2004).
- [23] M. A. Abramowitz and L. A. Stegun, *Handbook of Mathematical Functions and Formulas, Graphs and Mathematical Tables* (Dover Publications, New York, 1972).
- [24] P. C. Hendry, P. V. E. McClintock, H. A. Nichol, L. Skrbek, and W. F. Vinen, *J. Low Temp. Phys.* **138**, 543 (2005).
- [25] D. Charalambous, P. C. Hendry, P. V. E. McClintock, L. Skrbek, and W. F. Vinen, in *Proceedings of the 24th International Conference on Low Temperature Physics* (AIP, Melville, NY, 2006), pp. 205–206.
- [26] R. J. Donnelly and C. F. Barenghi, *J. Phys. Chem. Ref. Data* **27**, 1217 (1998).
- [27] H. Yano (private communication).
- [28] J. Jäger, B. Schuderer, and W. Schoepe, *Physica B* **210**, 201 (1995).
- [29] G. Baym, G. Barrera, and C. J. Pethick, *Phys. Rev. Lett.* **22**, 20 (1969).